A Solution Structure for Poly(rA)·Poly(dT) with Different Furanose Pucker and Backbone Geometry in rA and dT Strands and Intrastrand Hydrogen Bonding of Adenine 8CH†

J. M. Benevides and G. J. Thomas, Jr.*

Division of Cell Biology and Biophysics, School of Basic Life Sciences, University of Missouri—Kansas City, Kansas City, Missouri 64110

Received July 21, 1987; Revised Manuscript Received November 6, 1987

ABSTRACT: Equilibrium Raman spectra show that A- and B-form phosphodiester backbone geometries are both present in the solution structure of the RNA·DNA hybrid poly(rA)·poly(dT) and that these arise from *C3′-endo-rA* and *C2′-endo-dT* nucleosides, respectively. Raman dynamic measurement of deuterium exchange of adenine 8CH groups reveals (i) a *single* kinetic class of rA conformers and (ii) extraordinary retardation of 8CH exchange in this class—more than 100-fold slower than in canonical DNA structures. The equilibrium and kinetic results, in conjunction with model building, indicate an unusual intrastrand hydrogen bond involving adenosine donor (8C–H) and acceptor (5′O) groups and a double-helical conformation in solution similar to that proposed for fibers at high relative humidity [Zimmerman, S. B., & Pheiffer, B. H. (1981) *Proc. Natl. Acad. Sci. U.S.A. 78*, 78–82]. In fibers of poly(rA)·poly(dT) at low relative humidity, the Raman spectra indicate a conventional A-helix structure.

Hybrid nucleic acids containing a strand of RNA in association with a strand of DNA are important in a number of biological processes, including transcription and replication, and their structures have been investigated with various diffraction (Zimmerman & Pheiffer, 1981; Arnott et al., 1986; Wang et al., 1982) and spectroscopic techniques (Mellema et al., 1983; Shindo & Matsumoto, 1984; Fujiwara & Shindo, 1985; Benevides et al., 1986; Steely et al., 1986). The poly(rA)·poly(dT) structure has been probed in both fibers and solutions, and these studies have led to seemingly conflicting results on nucleoside sugar puckers and phosphodiester backbone geometries in the two strands (Zimmerman & Pheiffer, 1981; Gupta et al., 1985). On the basis of fiber X-ray diffraction, Zimmerman and Pheiffer (1981) proposed that the hybrid at high relative humidity (92% RH) exhibited structural similarities to B-DNA. Model building indicated this structure was likely to contain a poly(dT) strand of the B form with C3′-*exo*-deoxyribosyl ring pucker (i.e., C2′-endo family pucker) and a poly(rA) strand of the A form with C3′-*endo*-ribosyl pucker. The diffraction calculated from the proposed model was found to be in good agreement with the observed fiber pattern. These authors also found that at lower RH (75%) poly(rA)·poly(dT) yielded the diffraction pattern characteristic of a conventional 11-fold A-RNA helix. [We use the designations A and B in their usual context for RNA and DNA conformations. Structural characteristics associated with the A form are 11-fold helix pitch, C3′-endo family sugar pucker, significant base tilt (~15°), and phosphodiester torsion angles (α, ζ) in the range (−70 ± 20, −65 ± 20°). In the B form the corresponding characteristics are typically 10.5-fold helix, C2′-endo family pucker (including C3′-exo, C1′-exo, or occasionally O4′-endo), lesser base tilt, and (α, ζ) = (−50 ± 10, −120 ± 30°).]

Solid-state ^{31}P NMR results obtained on fibers of poly(rA)·poly(dT) have confirmed the conformational transition induced by hydration at about 90% RH (Shindo & Matsumoto, 1984; Fujiwara & Shindo, 1985). The NMR data were interpreted as indicative of a heterogeneous population of phosphorus groups at high RH and a homogeneous population at low RH. Although the ^{31}P resonances reflect only the magnetic environment of the backbone phosphodiester groups, they appear to be consistent with the model proposed by Zimmerman and Pheiffer (1981). In apparent conflict with the above studies, Gupta et al. (1985) recently concluded from solution NMR–NOE (nuclear Overhauser effect) data that poly(rA)·poly(dT) lacks C3′-endo sugars in the rA strand. The latter authors have proposed instead a model for the hybrid which incorporates C1′-exo sugar pucker (i.e., C2′-endo family) in both strands.

Recently, we (Thomas et al., 1986) and others (Katahira et al., 1986; Taillandier et al., 1987) have published Raman spectra of the hybrid in solution. The equilibrium Raman data indicate for the solution structure a duplex of the "heteronomous" type (Arnott et al., 1986), which appears to be consistent with the results obtained from fiber X-ray diffraction at high RH. However, on the basis of the equilibrium Raman results alone a detailed molecular model for the solution structure of poly(rA)·poly(dT) cannot be inferred. To provide additional constraints for model building we have obtained and interpreted the hydrogen isotope exchange kinetics of the adenine 8CH groups in this hybrid structure. The Raman dynamic measurements serve as a specific probe of solvent accessibility to the purine 7N and 8C ring sites and can be interpreted by analogy with model compound studies to also yield information concerning the overall topological characteristics of the helix grooves (Benevides & Thomas, 1985). Here we report a model for the solution structure of poly(rA)·poly(dT) which accounts for both the equilibrium and dynamic Raman results and is consistent with the X-ray and NMR data obtained by others.

Polynucleotides and their complexes have been extensively studied by Raman spectroscopy in the past decade, and comprehensive reviews have been given (Thomas, 1986; Peticolas et al., 1987). The Raman lines characteristic of different nucleic acid conformations permit the differentiation of A, B,

† This research was supported by NIH Grant AI18758. This is paper 33 in the series "Raman Spectral Studies of Nucleic Acids". Paper 32 in this series is Benevides et al. (1988).

* Author to whom correspondence should be addressed.

0006-2960/88/0427-3868$01.50/0

Table I: Raman Lines (cm^{-1}) Characteristic of Nucleic Acid Backbone Geometry[a]

A-DNA	A-RNA	B-DNA	assignment
705 ± 2	712 ± 3		main chain
		784 ± 3	OPO symmetric stretch
807 ± 2	812 ± 3		OPO antisymmetric + symmetric stretch
		832 ± 7	OPO antisymmetric stretch
1099 ± 2	1099 ± 2	1092 ± 2	PO_2^- symmetric stretch
1418 ± 2	1419 ± 2	1422 ± 2	CH_2 deformation

[a] Basis for assignments is discussed in Prescott et al. (1984) and Thomas et al. (1986).

Table II: Selected Conformation-Sensitive Raman Lines (cm^{-1}) of Thymidine and Adenosine[a]

C2′-endo/anti	dA	663 ± 2
	dT	668 ± 2
	dT	748 ± 2
	dT	1142 ± 2
	dT	1208 ± 2
C3′-endo/anti	dA or rA	644 ± 4
	dT	668 ± 2[b]
	dT	745 ± 2[c]
	dT	777 ± 2
	dT	1239 ± 2

[a] Basis for assignments is discussed in Thomas et al. (1986) and Thomas and Benevides (1985). [b] Very low intensity compared to 668-cm^{-1} line of C2′-endo isomer, above. [c] Very low intensity compared to 748-cm^{-1} line of C2′-endo isomer, above.

and Z backbone geometries and the identification of C2′-endo and C3′-endo families of nucleoside sugar pucker and of *syn*- and *anti*-glycosyl bond orientations (Benevides & Thomas, 1983; Prescott et al., 1984; Benevides et al., 1984a, 1986, 1988). Of present interest are several Raman bands associated with vibrations localized in the phosphodiester (OPO) and phosphodioxy (PO_2^-) groups, referred to as Raman markers of A- and B-DNA backbone geometries and summarized in Table I. Also of interest are Raman bands associated with specific nucleoside base and sugar conformations, which are summarized in Table II.

Experimental Procedures

The following polynucleotides were obtained from Pharmacia P-L Biochemicals: poly(dA-dT)·poly(dA-dT) (lot 658/92), poly(rA)·poly(dT) (lot 675-81), and poly(dA) (lot 658/42). Poly(rA) (lot P-9403) was obtained from Sigma Chemical Co. All polynucleotides were dissolved to a concentration of 40 mg/mL in 0.1 M NaCl solution at pH 7.5 for Raman spectroscopy. Similar solutions were prepared at pD 7.5 with D_2O (99.8%, Aldrich Chemical Co.) as solvent. Fibers of poly(dA-dT)·poly(dA-dT), poly(rA)·poly(dT), and poly(dA) were drawn from H_2O solutions and were maintained in hygrostatic cells for laser Raman excitation according to procedures described in detail elsewhere (Prescott et al., 1984). In all cases where D_2O was employed as the solvent, the polynucleotide was first lyophilized from D_2O to minimize protium contamination.

Spectra were excited with the 514.5-nm line of an argon laser (Coherent Innova 70-2) using 200–300 mW of radiant power at the sample. Raman scattering at 90° was collected and analyzed on a Spex Ramalog spectrometer under the control of a North Star Horizon-II microcomputer (Li et al., 1981). Spectral data were collected at intervals of 1.0 cm^{-1}, with an integration time of 1.5 s and a spectral slit width of 8.0 cm^{-1}. All data collected from the solutions or fibers were corrected for Raman scattering of the aqueous solvent (H_2O or D_2O) as described previously (Thomas & Benevides, 1985; Benevides et al., 1986). Each spectrum shown is the average of several scans.

Protocols for deuterium exchange of purine 8CH groups of poly(rA)·poly(dT) were as described by Benevides et al. (1984b), using quantitative Raman spectrophotometry (Thomas & Livramento, 1975). Briefly, Raman cells containing the polynucleotide in D_2O were incubated at the temperature selected for exchange (50 ± 0.1 °C). Sample cells were removed periodically from the incubator and thermostated at low temperature (10 °C) to effectively arrest exchange while spectral data were being collected. The spectra were scanned to monitor both the exchange-sensitive Raman lines between 1400 and 1500 cm^{-1} and the internal Raman intensity standard near 1094 cm^{-1}. As exchange progresses, the Raman intensity of the 8CH isotopomer near 1480 cm^{-1} decreases, and a concomitant increase in intensity occurs near 1460 cm^{-1} which is attributable to formation of the 8CD isotopomer. The integrity of the hybrid double helix at the exchange temperature (50 °C) was established prior to the start of exchange and monitored both by Raman and UV spectra, which showed no loss of hypochromism or band shifts.

The pseudo-first-order rate constant governing 8CH exchange at temperature T was determined from

$$k(T) = (1/t) \ln [(I^0 - I^\infty)/(I^t - I^\infty)]$$

where I^0, I^∞, and I^t are the normalized intensities of the exchange-sensitive Raman line at times zero, infinity, and t, respectively. The pseudo-first-order rate constant was then utilized to calculate the retardation factor (R), which is defined as the ratio of exchange rates of mononucleotide (5′ rAMP) and poly(rA)·poly(dT) (Benevides & Thomas, 1985). Further details of instrumentation, sample handling, data collection, signal averaging, and Fourier deconvolution techniques are described in previous publications [Thomas (1986) and references cited therein].

Results and Discussion

Equilibrium Raman Spectra. The Raman spectrum of aqueous poly(rA)·poly(dT) is shown in Figure 1 (top), where it is compared with Raman spectra of model B-DNA [poly(dA-dT)·poly(dA-dT) solution] and model A-DNA [poly(dA-dT)·poly(dA-dT) fiber] structures, which contain the same base composition (Assa-Munt & Kearns, 1984; Thomas & Benevides, 1985). The spectrum of the poly(rA)·poly(dT) fiber obtained at 95% RH, not shown in Figure 1, exhibits no discernible differences from the solution spectrum.

The spectrum of aqueous poly(dA-dT)·poly(dA-dT) exhibits phosphodiester group Raman markers at 791, 839, and 1092 cm^{-1}, as expected from its B-form backbone. The fiber of poly(dA-dT)·poly(dA-dT) at 75% RH exhibits corresponding Raman markers at 705, 806, and 1099 cm^{-1}, as expected from its A-form backbone (Table I). Thus, the data of Figure 1 clearly reveal the presence of *both* A-type and B-type phosphodiester backbone geometries in the solution structure of the hybrid, and the relative intensities are consistent with a 1:1 ratio of A and B conformers. The location of the PO_2^- Raman marker at 1094 cm^{-1} in the hybrid, i.e., at nearly the same frequency observed for B-DNA and well removed from that for A-DNA (1099 cm^{-1}, Table I), is evidence of a more B-like configuration for phosphate groups of the hybrid structure. This could explain the results of netropsin binding studies (Wartell et al., 1974). Nonetheless, the foregoing Raman data show that poly(rA)·poly(dT) is not a typical B family structure, and this is confirmed by isotopic hydrogen exchange measurements discussed below.

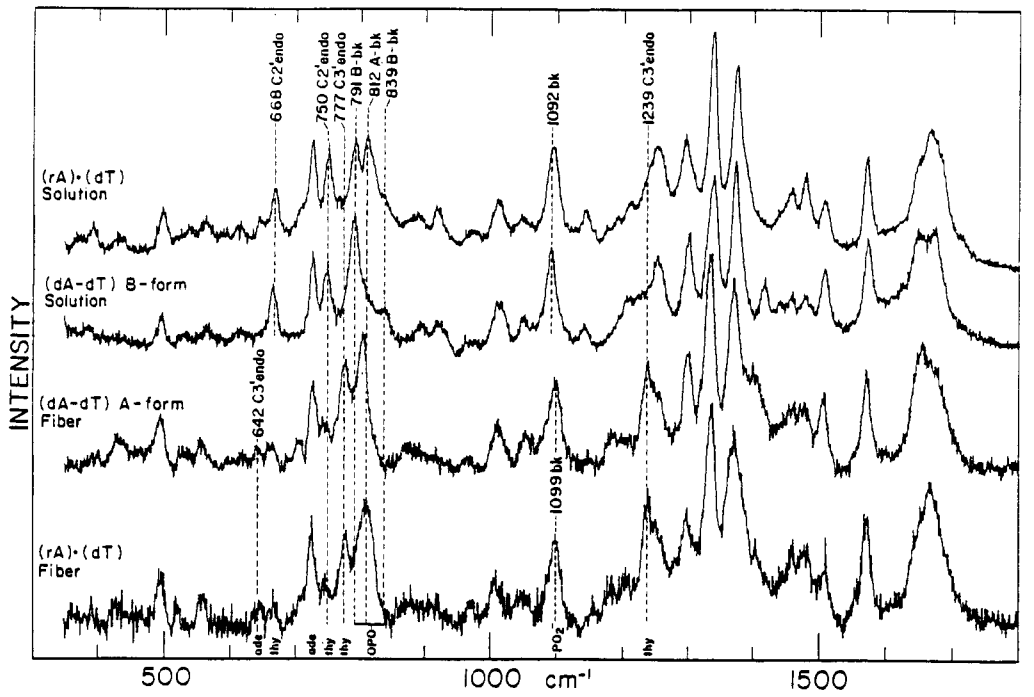

FIGURE 1: Raman spectra in the region 300–1800 cm^{-1} obtained with Ar^+ 514.5-nm excitation. From top to bottom: solution of poly(rA)·poly(dT), pH 7.5 in 0.1 M NaCl; solution of poly(dA-dT)·poly(dA-dT), pH 7.5 in 0.1 M NaCl; fiber of poly(dA-dT)·poly(dA-dT) at 75% RH; fiber of poly(rA)-poly(dT) at 75% RH. Each spectrum is the average of several scans and is corrected for background scattering of solvent.

In addition to the characteristic Raman backbone markers identified above (Table I), a number of Raman bands originating from vibrations of the purine or pyrimidine residues, and mechanically coupled to vibrational modes of the furanose ring, can serve as indicators of specific nucleoside sugar ring pucker. In particular, several vibrational modes of dT are highly sensitive to furanose conformation (Thomas & Benevides, 1985; Thomas et al., 1986). The corresponding Raman marker bands are listed in Table II. Inspection of Figure 1 and Table II shows that the hybrid poly(rA)·poly(dT) in solution contains the key Raman markers (668 and 750 cm^{-1}) diagnostic of C2′-*endo*/*anti*-thymidine and, in addition, lacks those markers (777 and 1239 cm^{-1}) associated with C3′-*endo*/*anti*-thymidine. These data show that the geometry of the poly(dT) strand of the hybrid is of the B form. It follows that the A-form component of the hybrid is the poly(rA) strand.

Support for this interpretation is provided by the band near 645 cm^{-1} in the solution spectrum of the hybrid, which can be assigned to C3′-endo conformers of rA on the basis of the following evidence. A band near 645 ± 5 cm^{-1} is always detected in Raman spectra of polynucleotides and mononucleotides containing C3′-endo conformers of adenosine or deoxyadenosine. Examples include the low-RH fiber of poly(dA-dT)·poly(dA-dT) [see Figure 1 and Thomas and Benevides (1985)], the low-RH fiber of poly(dA) (Figure 2), aqueous poly(rA) (Figure 2), complexes of poly(rA) with poly(rU) (Lafleur et al., 1972; Morikawa et al., 1973), and 5′ rAMP (Lord & Thomas, 1967). Figure 2 also shows that the adenosine band shifts to ca. 663 cm^{-1} when the sugar pucker is changed to the C2′-endo family as in aqueous poly(dA).

The 645-cm^{-1} band observed in low-RH fibers of poly(dA-dT)·poly(dA-dT) had been assigned previously to dT residues (Thomas & Benevides, 1985). The present data show (i) that dA and rA residues with C3′-endo sugar pucker also contribute Raman intensity near 645 cm^{-1}, even in the absence of dT residues, and (ii) that the adenine band shifts to higher frequency with the change of pucker from C3′-endo to C2′-endo

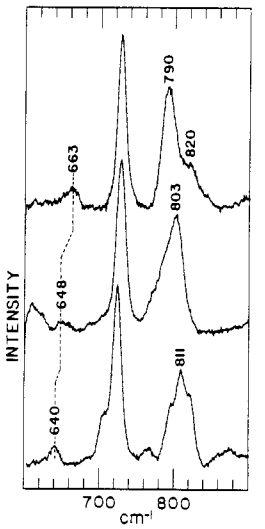

FIGURE 2: Raman spectra of polyadenylates in the region 600–900 cm^{-1}. (Top) Solution of poly(dA) at pH 7.5 in 0.1 M NaCl. (Middle) Fiber of poly(dA) at 75% RH. (Bottom) Solution of poly(rA) at pH 7.5 in 0.1 M NaCl. The vertical dashed line indicates the position of the adenosine nucleoside conformation marker discussed in the text. Conformation-sensitive bands of the backbone are also labeled. [See text and Thomas et al. (1986) for discussion.]

(Figure 2). Both the magnitude and direction of the frequency shift in this adenine marker band parallel those observed for the guanine marker band of DNA (Benevides et al., 1988). The new results are included in Table II.

Previously, we reported Raman spectra obtained from fibers of poly(rA)·poly(dT) equilibrated at low (75%) RH, for comparison with RNA and DNA oligonucleotide crystals (Thomas et al., 1986). The low-RH fiber spectrum, reproduced in Figure 1 (bottom), shows that only the A-backbone geometry and only C3′-endo/anti nucleosides (both rA and dT) are present at these conditions. The Raman results demonstrate that the reported fiber X-ray diffraction (Zimmerman & Pheiffer, 1981) and ^{31}P NMR spectra (Shindo & Matsumoto, 1984) are those of a conventional A-form

structure and that this A-form structure at low RH is fundamentally different from the structure which prevails in solution or in fibers at high RH.

Hydrogen–Deuterium Exchange. Although the data of Figure 1 indicate phosphodiester geometries of the A form in the adenylate strand and of the B form in the thymidylate strand of aqueous poly(rA)·poly(dT), the equilibrium Raman spectra do not provide detailed information on the overall topological characteristics of the poly(rA)·poly(dT) double helix, such as major and minor groove features which are potentially significant for protein recognition and solvent stabilization of secondary structure. Groove dimensions may also influence molecular packing, to which X-ray and ^{31}P NMR data are sensitive (Zimmerman & Pheiffer, 1981; Shindo & Matsumoto, 1984). In order to obtain further information on solvent accessibility to the major groove, we have examined deuterium isotope exchange of purine 8CH groups in aqueous poly(rA)·poly(dT). The kinetics of deuterium exchange of nucleic acid 8CH groups, which depend upon solvent penetration to the purine 7N–8C locus (Tomasz et al., 1972), are conveniently measured by Raman spectrophotometry (Thomas & Livramento, 1975). The exchange rate can thus be exploited as a sensitive indicator of major groove features of DNA and RNA, and specifically to reveal hydrogen bonding to the purine 7N acceptor (Benevides & Thomas, 1985). Among conventional nucleic acid secondary structures, we have found that the rate of exchange decreases, i.e., retardation of exchange increases, in the order Z-DNA < ss-DNA = ss-RNA < ds-B-DNA < ds-A-RNA < ms-A-RNA. (Here, ss, ds, and ms refer to single-stranded, double-stranded, and multistranded structures, respectively.) When compared with mononucleotides, nucleic acid 8CH exchange is retarded approximately 3-fold in B-DNA, approximately 10-fold in A-RNA, and more than 200-fold in triplex and quadruplex structures which contain Hoogsteen-type hydrogen bonding at adenine or guanine 7N sites (Benevides & Thomas, 1985). By measuring the deuterium exchange rate of rA residues in poly(rA)·poly(dT), we hoped to determine whether the environment at 7N–8C more closely approximated that of B-DNA (2.5–4-fold retardation) or A-RNA (5–10-fold retardation). The procedures for measuring the exchange kinetics have been described in detail elsewhere (Thomas & Livramento, 1975; Benevides et al., 1984b; Benevides & Thomas, 1985) and are summarized under Experimental Procedures.

For poly(rA)·poly(dT) no exchange was detected after 30 days at 50 °C, which corresponds to a retardation factor at least as great as that in Hoogsteen paired structures (>200). To explain this unanticipated result, we investigated directly the possibility of Hoogsteen base pairing by ^1H NMR–NOE experiments on oligomeric (rA)·(dT) complexes. The observed NOE data unambiguously confirmed the presence of only Watson–Crick base pairs and only 1:1 stoichiometry of rA:dT, as will be reported elsewhere (Katahira et al., 1988). Therefore, the retardation of 8CH exchange in poly(rA)·poly(dT) does not arise from Hoogsteen pairing in the duplex nor from addition of a third strand [poly(dT)] forming hydrogen bonds to 7N acceptor sites of rA. Triple-strand formation, which is known to retard 8CH exchange in other polynucleotides (Benevides & Thomas, 1985), is considered unlikely in this case because all available data indicate that poly(rA)·poly(dT) cannot add an additional poly(dT) strand, even at salt concentrations much higher than employed here (Zimmerman & Pheiffer, 1981; Howard & Miles, 1984). Further, triplex formation would require disproportionation

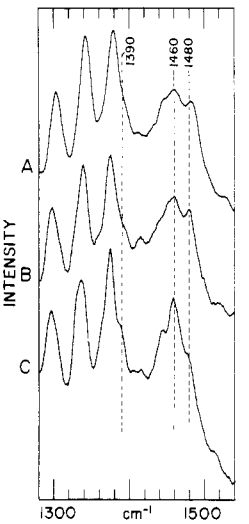

FIGURE 3: Raman spectra recorded at 10 °C from D_2O solutions of poly(rA)·poly(dT) in the region 1280–1540 cm^{-1}, showing bands sensitive to deuterium exchange of adenine 8CH groups. (A) Poly(rA)·poly(dT) in D_2O, before initiation of deuterium exchange (t = 0). (B) Poly(rA)·poly(dT) after incubation for 720 h in D_2O at 50 °C. The virtual identity of this spectrum to that at t = 0 indicates the absence of any significant deuterium exchange [cf. also Figure 3 of Thomas and Livramento (1975)]. (C) Poly(rA)·poly(dT) incubated as in (B), then subjected to strand dissociation at 70 °C, and further incubated for 24 h in D_2O at 70 °C. The resultant intensity changes at 1480, 1460, and 1390 cm^{-1} reflect 8C deuteriation in single-stranded poly(rA). [Note that spectral dissimilarities between Figure 3A and the corresponding region in Figure 1 (top) are a consequence of adenine $6NH_2$ and thymine 3NH deuteriation and do not result from any conformational differences. See also Benevides and Thomas (1985).]

of a poly(rA) strand which would be easily detected by its more rapid 8CH exchange. A rapidly exchanging ss-poly(rA) fraction was detected only at temperatures above the melting transition of poly(rA)·poly(dT) (T_m = 63 °C), as indicated in Figure 3. Evidently, another type of molecular interaction restricts solvent access to the 7N–8CH network in rA residues of poly(rA)·poly(dT). A candidate is hydrogen bonding of the 8CH group itself. Molecular model building indicates such hydrogen bonding to be consistent with both the Raman spectra and the NMR and fiber X-ray diffraction data.

We have built a model for the solution structure of poly(rA)·poly(dT) (Figure 4) using the following experimentally determined constraints: (i) Adenylate and thymidylate strands contain respectively C3′-endo and C2′-endo nucleoside sugar puckers, or closely related isomorphs, in agreement with the Raman spectral results. (ii) Bases are maintained near to perpendicularity with the helix axis in agreement with fiber diffraction results. This is supported indirectly by netropsin binding studies and directly by PO_2^- Raman markers which imply axial rise per residue and phosphodioxy group geometry similar to those of B-DNA. (iii) A third strand [poly(dT)] cannot be fitted to the duplex in accord with stoichiometric mixing curves and the absence of disproportionation. (iv) The pseudoacidic hydrogen attached to 8C of rA is sufficiently close to the phosphodiester backbone to sterically restrict solvent access to the 7N–8CH locus. This constraint also permits direction of the 8C–H bond toward a potential hydrogen-bond acceptor, namely, 5′O. Although H attached to C is not normally considered a hydrogen-bond donor, such a role has been proposed previously between purinic 8C–H and 5′O groups (Saenger, 1984). The occurrence of 8C–H···O5′ hydrogen bonding could restrict deuterium exchange of the 8CH proton and is consistent with the molecular model shown in Figure 4, where the 8C to 5′O distance is 3.02 Å. Since

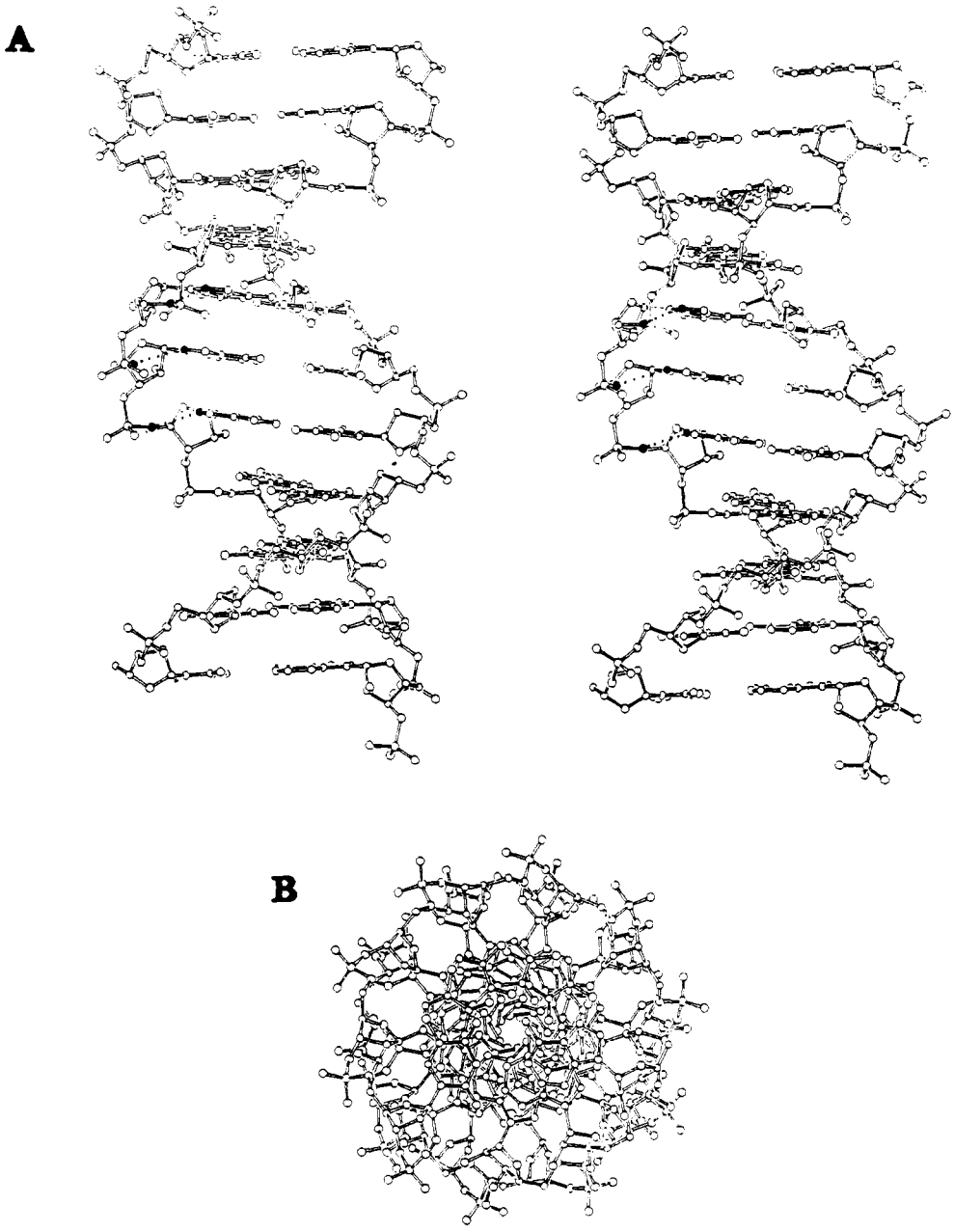

FIGURE 4: (A) Stereo drawing of the proposed solution structure of poly(rA)·poly(dT), based on published coordinates (Zimmerman & Pheiffer, 1981) and optimized for conformational properties determined from the Raman spectra, as discussed in the text. The view is approximately perpendicular to the helix axis and into the major groove. Lines connecting nonbonded atoms of the rA backbone (left strand) indicate proposed 8C–H to 5′O contacts for the central three adenylate residues. (B) View down the helix axis showing the proximity of the bases to the axis, typical of B-form nucleic acids.

Raman spectra of the poly(rA)·poly(dT) solution and high-RH fiber are not distinguishable, we propose the model of Figure 4 also for the high-RH fiber structure. This model exhibits some similarities to that proposed by Zimmerman and Pheiffer (1981) but differs in the more conventional C2′-endo pucker of dT and the closer approach of 8C–H to the adenylyl 5′O atom.

CONCLUSIONS

The equilibrium Raman results show clearly that the solution structure of poly(rA)·poly(dT) is a true hybrid in which the poly(rA) chain contains C3′-endo sugar pucker and an A-type phosphodiester geometry, while the poly(dT) strand exhibits C2′-endo pucker (or a minor variation thereof) and a B-like phosphodiester backbone. In our model, a third strand cannot be added because of steric hindrance between the 2C=O oxygen of the resident dT strand and the backbone of the poly(rA) strand. This is a direct consequence of the interstrand difference in nucleoside sugar pucker. In our view, it is not likely that a triple-stranded complex could form unless the puckers of both polypyrimidine strands were converted to C3′-endo. This conclusion is consistent with recent CD studies of hybrid AT and AU polynucleotide complexes (Steely et al., 1986). The Raman dynamic results show that the hybrid structure exhibits the purine 8CH exchange kinetics of neither A-form nor B-form nucleic acids but suffers instead severe retardation of 8CH exchange. Similar retardation has been observed only in polynucleotides containing purine 7N hydrogen bonding; yet no evidence exists for base pairing in poly(rA)·poly(dT) that would utilize the 7N site. Model building suggests that the restricted exchange results from direct hydrogen bonding between 8C–H as donor and 5′O as acceptor in each nucleotide along the rA strand. The present results indicate also that the global geometry of the solution

structure resembles that of B-DNA, in that the bases are close to the helix axis, in general accord with the Zimmerman and Pheiffer fiber model.

The present results show that the Raman spectrum contains a band diagnostic of adenosine sugar ring pucker in the 640–665-cm^{-1} interval. However, the band is intrinsically weak, and its position overlaps with that of dG and dT markers, rendering it of limited usefulness for accessing deoxyadenosine sugar conformations in DNA.

Recently, a number of hybrid oligomer crystal structures have been solved by X-ray methods. Spectroscopic examination of the solution structures of two of these, r(GCG)d(TATACGC) and r(GCG)d(CGC), has indicated that the energetically preferred conformations of ribo (C3′-endo) and deoxyribo sugars (C2′-endo) are able to coexist in the solution structures, even though only one conformer prevails in the lower water environment of the crystal (Wang et al., 1982; Mellema et al., 1983; Benevides et al., 1986). Our findings on poly(rA)·poly(dT) are consistent with the hybrid oligomer results: Both families of sugar pucker are present in the solution structure, but only one type of conformer, viz., C3′-endo, occurs when the activity of water is reduced in the low-RH fiber. The present study also shows that the two families of sugar conformations may be well accommodated in opposing strands of a double helix in solution, as required in a transcription complex.

ACKNOWLEDGMENTS

We thank Andrew H.-J. Wang and Juan Aymami of MIT for providing computer graphics facilities and for useful comments on the manuscript.

Registry No. Poly(rA)·poly(dT), 27156-07-6.

REFERENCES

Arnott, S., Chandrasekaran, R., Millane, R. P., & Park, H.-S. (1986) *J. Mol. Biol. 188*, 631–640.

Assa-Munt, N., & Kearns, D. R. (1984) *Biochemistry 23*, 791–796.

Benevides, J. M., & Thomas, G. J., Jr. (1983) *Nucleic Acids Res. 11*, 5747–5761.

Benevides, J. M., & Thomas, G. J., Jr. (1985) *Biopolymers 24*, 667–682.

Benevides, J. M., Wang, A. H.-J., van der Marel, G. A., van Boom, J. H., Rich, A., & Thomas, G. J., Jr. (1984a) *Nucleic Acids Res. 12*, 5913–5925.

Benevides, J. M., LeMeur, D., & Thomas, G. J., Jr. (1984b) *Biopolymers 23*, 1011–1024.

Benevides, J. M., Wang, A. H.-J., Rich, A., Kyogoku, Y., van der Marel, G. A., van Boom, J. H., & Thomas, G. J., Jr. (1986) *Biochemistry 25*, 41–50.

Benevides, J. M., Wang, A. H.-J., van der Marel, G. A., van Boom, J. H., & Thomas, G. J., Jr. (1988) *Biochemistry 27*, 931–938.

Fujiwara, T., & Shindo, H. (1985) *Biochemistry 24*, 896–902.

Gupta, G., Sarma, M. H., & Sarma, R. H. (1985) *J. Mol. Biol. 186*, 463–469.

Howard, F. B., & Miles, H. T. (1984) *Biochemistry 23*, 6723–6732.

Katahira, M., Nishimura, Y., Tsuboi, M., Sato, T., Mitsui, Y., & Iitaka, Y. (1986) *Biochim. Biophys. Acta 867*, 256–266.

Katahira, M., Kyogoku, Y., Benevides, J. M., & Thomas, G. J., Jr. (1988) *Nucleic Acids Res.* (submitted for publication).

Lafleur, L., Rice, J., & Thomas, G. J., Jr. (1972) *Biopolymers 11*, 2432–2437.

Lord, R. C., & Thomas, G. J., Jr. (1967) *Spectrochim. Acta, Part A 23A*, 2551–2591.

Li, Y., Thomas, G. J., Jr., Fuller, M., & King, J. (1981) *Prog. Clin. Biol. Res. 64*, 271–283.

Mellema, J.-R., Haasnoot, C. A. G., van der Marel, G. A., Willie, G., van Boeckel, C. A. A., van Boom, J. H., & Altona, C. (1983) *Nucleic Acids Res. 11*, 5717–5738.

Morikawa, K., Tsuboi, M., Takahashi, S., Kyogoku, Y., Mitsui, Y., Iitaka, Y., & Thomas, G. J., Jr. (1973) *Biopolymers 12*, 799–816.

Peticolas, W. L., Kubasek, W. L., Thomas, G. A., & Tsuboi, M. (1987) in *Biological Applications of Raman Spectroscopy* (Spiro, T. G., Ed.) Vol. 1, pp 81–133, Wiley, New York.

Prescott, B., Steinmetz, W., & Thomas, G. J., Jr. (1984) *Biopolymers 23*, 235–256.

Saenger, W. (1984) in *Principles of Nucleic Acid Structure* (Cantor, C. R., Ed.) pp 51–104, Springer-Verlag, New York.

Shindo, H., & Matsumoto, U. (1984) *J. Biol. Chem. 259*, 8682–8684.

Steely, H. T., Jr., Gray, D. M., & Ratliff, R. L. (1986) *Nucleic Acids Res. 14*, 10071–10090.

Taillandier, E., Ridoux, J.-P., Liquier, J., Leupin., W., Denny, W. A., Wang, Y., Thomas, G. A., & Peticolas, W. L. (1987) *Biochemistry 26*, 3361–3368.

Thomas, G. J., Jr. (1986) in *Advances in Spectroscopy* (Clark, R. J. H., & Hester, R. E., Eds.) Vol. 13, pp 233–309, Wiley, New York.

Thomas, G. J., Jr., & Livramento, J. (1975) *Biochemistry 14*, 5210–5218.

Thomas, G. J., Jr., & Benevides, J. M. (1985) *Biopolymers 24*, 1101–1105.

Thomas, G. J., Jr., Prescott, B., & Benevides, J. M. (1986) *Biomol. Stereodyn. 4*, 227–254.

Tomasz, M., Olson, J., & Mercado, C. M. (1972) *Biochemistry 11*, 1235–1241.

Wang, A. H.-J., Fujii, S., van Boom, J. H., van der Marel, G. A., van Boeckel, S. A., & Rich, A. (1982) *Nature (London) 299*, 601–604.

Wartell, R. M., Larson, J. E., & Wells, R. D. (1974) *J. Biol. Chem. 49*, 6719–6731.

Zimmerman, S. B., & Pheiffer, B. H. (1981) *Proc. Natl. Acad. Sci. U.S.A. 78*, 78–82.